ASME 2012 5th Annual Dynamic Systems and Control Conference joint with the JSME 2012 11th Motion and Vibration Conference
DSCC2012-MOVIC2012
October 17-19, 2012, Fort Lauderdale, Florida, USA

DSCC2012-MOVIC2012-8694

PEDESTRIAN AVOIDANCE FOR UNMANNED GROUND VEHICLES BASED ON VELOCITY OCCUPANCY SPACE

William J. Westrick*
Department of Mechanical Engineering
University of Michigan
Ann Arbor, MI 48109-2125
Email: westricw@umich.edu

A. Galip Ulsoy
Huei Peng
Department of Mechanical Engineering
University of Michigan
Ann Arbor, MI 48109-2125

ABSTRACT

Velocity Occupancy Space (VOS) is an algorithm used to perform real-time moving obstacle avoidance for Unmanned Ground Vehicles (UGVs). Pedestrian safety and comfort must be ensured by the guidance algorithm when UGVs operate near pedestrians. Studies on human interactions are used to formulate desired behavior of the UGV as it avoids people. Then, VOS is enhanced with improved avoidance behavior. We investigate three potential methods for enhancing pedestrian safety and comfort. To study the effect of these enhancements, numerical simulations of a large set of randomly generated scenarios. The number of collisions, and minimum required opening width, were used to characterize the performance of each avoidance enhancement technique. Two of the methods eliminate collisions with pedestrians; the preferred technique, which artificially enlarges the size of detected pedestrians, accomplishes this consistently.

INTRODUCTION

Summary

Velocity Occupancy Space (VOS) is an obstacle avoidance technique developed by Bis et al. [1,2] for use with mobile robots that have sensor uncertainties. This paper focuses on characterizing how VOS changes behavior as parameters are varied and how to adjust them in order to ensure pedestrian safety and comfort.

Literature Review

Human Comfort and Safety One of the key criteria for human interactions with robots is how safe and comfortable the person feels. This is a highly subjective set of criteria and the results vary from person to person. As the intention of this research is to operate a robot seamlessly among humans, it is assumed that behavior that mimics conservative human motion would be acceptable for the robot. A large amount of research has gone into studying the social interactions between people, and we use this knowledge as a driving motivation in modifying the obstacle avoidance algorithm to accommodate humans.

One of the most influential areas of research for human-robot social interaction is in proxemics, a concept discussed by Edward Hall [3,4] that concerns cultural preferences towards interpersonal distances. For example, interactions between 1.2 m to 3.6 m are preferred when conversing with non-friends [5]. Studies, such as those done by Walters et al., Oosterhout and Visser, Pacchierotti et al., and Koay et al., have looked at the application of proxemics to mobile robots [5,6,7,8].

Walters et al. found that "most participants kept interpersonal distances from the robot corresponding to Hall's Personal Spatial Zone (0.45 m to 1.2 m)" [5]. Oosterhout and Visser monitored two robots that interacted with visitors during a festival, and observed that interactions imply "acceptance of the robots as an agent that represents a social being," even if they did not know that the robots were controlled by humans [6]. Pacchierotti et al. examined hallway interactions from the perspective of path planning. For social interactions, they claimed that "avoidance must be initiated early enough to signal that the robot has detected the presence of a person and to indicate its intention to provide safe passage for him/her" [7]. This advance notice reduces human anxiety regarding a collision with an unfamiliar robot. From proxemics, Pacchierotti et al. determined that "one would expect the robot to initiate avoidance when the distance is about 3.5 m to the person. Given a need for reliable detection, limited dynamics, and early warning, however, a longer distance seems to be desir-

*Address all correspondence to this author.

able" [7]. This provides some insight into human preferences and the desired structure of human-robot interactions. Koay et al. use a custom device to monitor subjects' comfort as they interact with a robot. They also found that Hall's proxemics descriptions were reasonable as "the majority of subjects experienced discomfort when the robot was closer than 3 m," which coincides with the social zone of Hall's proxemics [8].

Walters et al. [5] also looked at preferences with regard to visual characteristics and height. They found that the person's comfort depends more on their preferences than the robot itself. For example, they showed that people that preferred a tall robot allowed all the robots they tested to approach closer than those that preferred small robots, regardless of the actual robot size. Oosterhout and Visser observed distances at which people interacted with the robots and categorized the results by gender and age, which showed significant differences. For example, their measurements showed that adult females preferred a much larger distance (232.9 cm) than adult males (93.5 cm) [6].

Research on human acceptable motion by service robots has resulted in a variety of conclusions on acceptable behavior. One group has developed a method for path planning that takes into account human acceptable motion [9]. The robot detects faces using vision to determine the direction that the human is facing and uses LIDAR to track motion. The path planning algorithm then takes into account the orientation of the human to avoid passing too closely behind or to the side– behaviors which make the human uncomfortable. The planner also takes into account whether the human is standing or sitting– a standing person is generally comfortable with closer interactions. The path planner developed by Sisbot et al. [9] develops a cost field that takes into account the human's field of view as well as safety to determine areas where the robot can move.

Additionally, research by Dongqing et al. compared approach distances and speeds (up to 4.5 m/s) using an unmanned Segway [10]. In their experiments, robots approached the subjects at various velocities, stopping at set distances, and the participants rated their perception of safety while their response was observed. At higher speeds (4.5 m/s), at both 1 m and 0.5 m stopping distances, the average response was that the system seemed slightly unsafe, with some participants even moving out of the way. When the robot performed the same trials at 2 m/s the average response was that the system seemed safe with no subjects moving out of the way. Their experiments show that people prefer interactions at moderate speeds which imply ample time to respond.

A number of studies have focused on human-human interactions in terms of passing or avoiding obstacles, and their application to robotics. Gérin-Lajoie et al. and Fink et al. studied human motion when avoiding obstacles in both real and virtual environments [11, 12]. Their research shows that the motion is nearly identical, and that the approach distance mimics Hall's proxemics concept. Following on the idea that human motion can be applied via mimicry to robotics, Yoda and Shiota [13] investigated human avoidance motion with the express interest of applying it to robotic motion. They studied the shape of the trajectory people

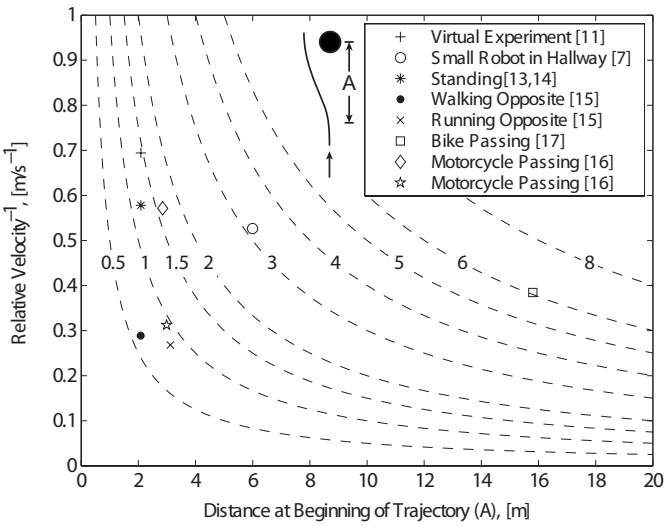

Figure 1: COMPARISON OF HUMAN INTERACTIONS WITH ROBOTS AND HUMANS. EACH POINT DESCRIBES THE BEGINNING OF THE AVOIDANCE MOTION. DASHED CURVES SHOW LINES OF CONSTANT TIME TO COLLISION.

took while navigating around another person. They found that the motion approximately followed a catenary, and used this in a path planner for a robot [13]. Then, Yoda and Shiota implemented the path planning into an actual robot and experimented with avoiding a person [14]. Butler and Agah [15] continued this idea and surveyed participants about their comfort while interacting with robots. They used a robot to mimic some human-like motion and found that "the smoother and more human-like movement of the non-stop passing was greatly preferred" [15].

Studies have also examined the interactions of bicyclists and motorcyclists. Minh et al. [16] monitored two intersections in Hanoi, Vietnam, and surveyed the behavior of the motorcyclists as they passed each other. They noticed that the average distance between the motorcycles before and after the passing procedure was 2.83 m to 2.87 m in exclusive motorcycle lanes with a relative speed of 6.3 km/h [16]. This equates to a 1.6 s time to collision (TTC), which is similar to human-human interactions. Khan and Raksuntorn [17] performed a similar study with bicyclists. They monitored a bicycle path and recorded interactions with passing bicycles. Their findings show an average passing length of 91.4 m with an average relative speed of 9.38 km/h. Assuming a symmetric trajectory, this can be translated into an average distance at the beginning and end of the passing procedure of 15.8 m, which equates to a 6.1 s TTC. This is much higher than human-human and motorcycle-motorcycle values (see Fig. 1). However, the bicycle path had no oncoming traffic. Without oncoming traffic there is less incentive to make the maneuver short. Hoffmann and Mortimer looked at estimation of TTC [18]. They found that for small TTCs, as is typical in human interactions, the TTC was typically underestimated. This underestimation means that drivers think they will crash earlier than they actually will, making them more cautious or increasing anxiety. In order to

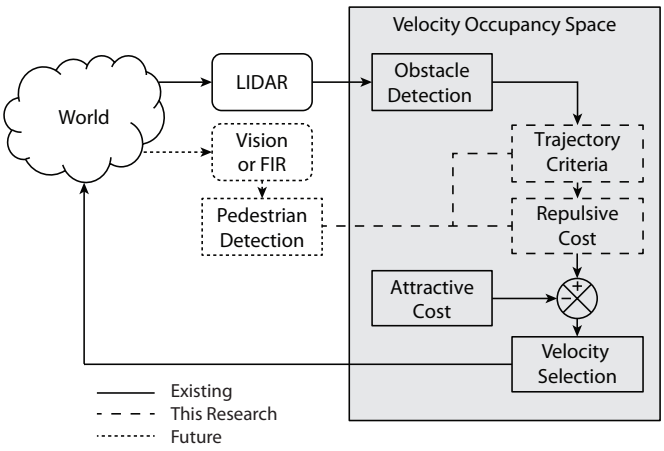

Figure 2: OVERVIEW OF VELOCITY OCCUPANCY SPACE.

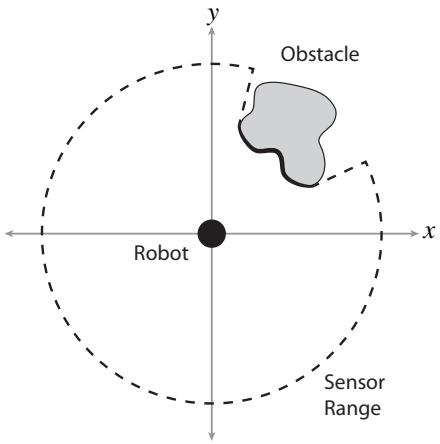

Figure 3: OBSTACLE DETECTION USING A 360° LIDAR. THIS FINDS THE EDGES OF THE OBSTACLE THAT FACE THE ROBOT, UP TO A LIMITED SENSOR RANGE.

alleviate this anxiety, the TTC should be kept large so it feels safe even after underestimation. Based on the TTC estimates found by Hoffmann and Mortimer, it would seem that a person's ability to estimate interactions are much better at closer distances, slower speeds, and lower TTCs. This could be a result of typical human interactions occurring in close proximity, at moderate speeds, and at low TTCs as shown in Fig. 1. This indicates that time to collision and distance are important in human interactions.

Pedestrian detection – and human detection in general – is a highly active field; a number of pedestrian detection algorithms and systems have been developed during the past decade. A number of field surveys and literature reviews have been published in the last five years, which shows just how broad and active the field has become, see [19, 20, 21] as examples. A variety of sensors are used in pedestrian detection; many systems use a visible or infrared camera, others use a stereo pair, and still others use LIDAR. One popular algorithm uses Histograms of Oriented Gradient descriptors to characterize images. It achieved as high as a 92% positive detection rate with a 1 per 5,000 false positive rate [22]. As such, this paper assumes that a pedestrian detection method is available for use by VOS.

Velocity Occupancy Space At a high-level, VOS operates by mapping detected obstacles into a velocity space [1, 2]. Then, VOS calculates the velocities that will lead to collisions. Additionally, VOS determines how quickly every reachable velocity would lead to the goal. A composite score is created for each velocity, taking into account the likelihood of collision and how quickly it leads to the goal. Finally, VOS selects the most favorable velocity at which the robot should move over the next time interval. A high-level description is presented in Fig. 2. VOS does not perform path planning over an extended period of time, therefore, it is intended to be used as a low-level, short time-horizon, regulator paired with a high level path-planning algorithm (e.g., A*) that would provide waypoints to define the overall desired motion.

Purpose and Scope

The purpose of this paper is to discuss the behavior of VOS around humans and investigate means of adjusting this motion to improve human comfort and safety. This is achieved by varying the repulsive weight applied to people. This repulsive weight translates into a different velocity choice, ideally leading the robot on a wider and safer trajectory around the person.

The second section of this paper will discuss the details of VOS and the repulsive weight components. The method in which VOS handles detected obstacles and specifics of trajectory selection will be described in order to evaluate potential areas for modification. Additionally, the simulator and scenarios used to evaluate the algorithm will briefly be described. Then, in the third section, three techniques will be presented for modifying VOS. The results of simulations using the the three techniques will be shown and evaluated. Finally, conclusions and areas for future work will be presented.

Background

Velocity Occupancy Space The first step in using VOS is to measure the environment and translate this into a map. This can be done using a variety of sensors. However, in this research, a LIDAR sensor is assumed to be used to provide a 360° view, as shown in Fig. 3. Readings from the sensor are translated into Cartesian coordinates centered on the robot. The coordinates are discretized and the resulting discrete configuration grid, subsequently referred to as the occupancy grid, is populated with the readings from the sensor, shown in Fig. 4. Once the occupancy grid has been populated by the readings from the sensor, the elements are grouped into discrete obstacles. These obstacles are tracked over time and a velocity estimate is made. Additionally, the occupancy grid is summed over multiple time steps, using a weighted sum, to account for sensor inconsistencies thereby taking into account missing and spurious detections. At this point, additional information from a pedestrian detection algorithm is assumed to be available and is used to determine the type of each

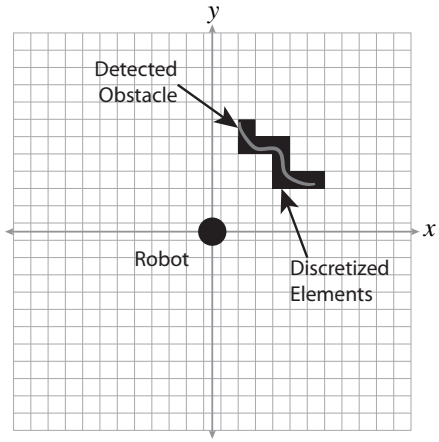

Figure 4: SENSOR READINGS TRANSLATED TO THE OCCUPANCY GRID. THE POINTS DETECTED BY THE SENSOR ARE DISCRETIZED AND USED TO FILL THE ELEMENTS OF THE OCCUPANCY GRID.

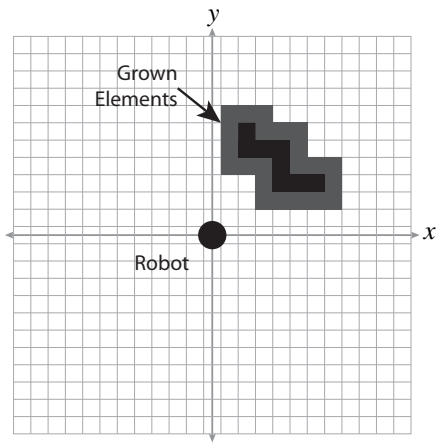

Figure 5: OCCUPANCY GRID AFTER ROBOT SIZE COMPENSATION.

obstacle. In the case of this research, the obstacles are predetermined to be either human or non-human. This information is used when computing the composite score or cost of each obstacle. By specifying the type of each obstacle, the relative importance can be adjusted between the obstacles when computing the cost and selecting appropriate velocities.

Once the occupancy grid has been populated and the obstacle velocities have been estimated, the obstacles are grown by filling in additional grid locations, as shown in Fig. 5. VOS treats the robot as a point, so to compensate, the obstacles are grown by the size of the robot. Once the grid has been fully populated with both detected elements and grown elements, they are mapped into velocity space. The velocity space is defined by the velocities that the robot can reach over the next time step. Each populated element in the occupancy grid is mapped into the velocity space by computing the velocity required by the robot in order to reach that element in one time step. Now, VOS must iterate through all of the reachable velocities and select a velocity for the next time step. For each reachable velocity, it must determine if that velocity will lead to any collisions with any of the obstacles in the future. This involves iterating over each of the populated elements in the occupancy grid, mapping each element into velocity space, and comparing the mapped velocity to the reachable velocity in question.

The relative velocity is compared with the relative position of the element to see if it would put the robot on a collision course. The velocity and position are vectors in the velocity space; if the vectors are aligned a collision could occur. The comparison is widened by an amount proportional to the distance to the element and the velocity uncertainty within the estimation. This widening and comparison was performed on the relative velocity vector by Bis et al. by checking the influence of the widening amount in each rectilinear direction and selecting the widest set [1,2]. In the course of implementing the VOS algorithm for the purposes of this research, the comparison technique was reformulated. The comparison was performed using vector cross products in order to save computation time and reduce programming complexity. An offset vector, $\vec{p}$ is constructed to be perpendicular to $\vec{v}_{rel}$ and of magnitude P_A, see Eq. 1. The offset vector is added and subtracted to the relative velocity vector to obtain two bound vectors for the comparison. A cross product is then performed between each bound vector and the relative position vector, and the sign is checked as shown in Eq. 2.

$$\vec{p} = \frac{\vec{v}_{rel}^{\perp}}{\|\vec{v}_{rel}\|} P_A \tag{1}$$

$$\begin{cases} \text{collision} & \text{if} \begin{cases} [\vec{\lambda}_i \times (\vec{v}_{rel} + \vec{p})] \cdot \hat{k} \leq 0 \text{ and} \\ [\vec{\lambda}_i \times (\vec{v}_{rel} - \vec{p})] \cdot \hat{k} \geq 0 \end{cases} \\ \text{no collision} & \text{otherwise} \end{cases} \tag{2}$$

The construction of P_A, therefore, has a significant impact on the comparison, as too small of a P_A will result in too few velocities being considered on a collision course. As such, P_A was constructed so that elements further away have a smaller offset and elements closer to the robot have a larger offset. The offset was also modulated by an adjustable weight, W_{AR}. The formulation used in this research is given in Eq. 3.

$$P_A = (1 - \frac{\|\vec{x}_i\|}{\text{Sensor Range}})^2 W_{AR} \tag{3}$$

This comparison to determine if a collision is possible is referred to in this paper as the 'trajectory criteria.' If the velocity is determined to lead to a collision at some point in the future, a cost calculation is performed for that element. This cost calculation takes into account the relative velocities, relative positions, obstacle type, and occupancy grid probability. In general, velocities leading to a collision sooner will have higher cost.

First, a value similar to time to collision (TTC_{VOS}) is calculated. This first involves checking if the occupied element is close enough that the robot velocity in question would reach it in less than one motor time step. If so, the TTC_{VOS} value is given a small value. Otherwise, the TTC_{VOS} is calculated by dividing

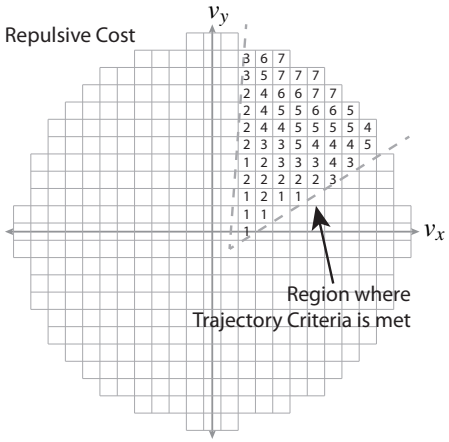

Figure 6: FINAL REPULSIVE COST FOR AN OBSTACLE.

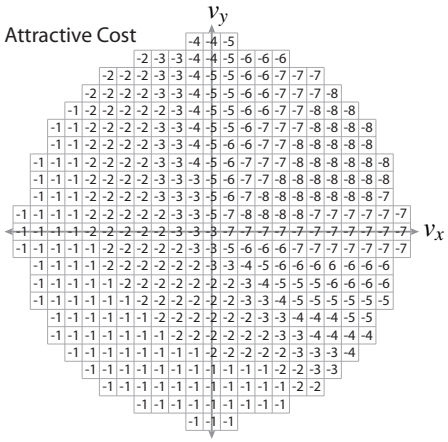

Figure 7: ATTRACTIVE COST TO MOVE THE ROBOT TOWARDS THE GOAL.

the relative position of the occupied element in velocity space by the relative velocity. The formulation used to calculate TTC_{VOS} is given in Eq. 4.

Additionally, the relative distance between the robot and the occupied element after the next time step is computed. This distance is squared when used for the score calculation. For programming safety, if the distance is zero, it is set to the resolution of the configuration grid– essentially the smallest unit of length recognizable by the algorithm. This pseudo-distance, CD, is given in Eq. 5.

$$TTC_{VOS,i} = \begin{cases} \dfrac{\left\|\vec{\lambda}_i\right\|}{\left\|\vec{v}_{rel}\right\|} & \text{if} \quad \|\vec{v}_r\| \leq \left\|\dot{\vec{x}}_i + \vec{\lambda}_i\right\| \\ \dfrac{\left\|\vec{\lambda}_i\right\|}{\text{Sensor Range}} & \text{otherwise} \end{cases} \tag{4}$$

$$CD_i = \begin{cases} \left\|\vec{\lambda}_i - \vec{v}_{rel}\right\|^2 & \text{if} \quad \left\|\vec{\lambda}_i - \vec{v}_{rel}\right\|^2 \neq 0 \\ res_c & \text{otherwise} \end{cases} \tag{5}$$

Once TTC_{VOS} and CD have been calculated, the score for that element is computed. TTC_{VOS} and CD are added together with a weight, W_{TTC}, to set their relative importance by multiplying TTC_{VOS}. This sum is then multiplied by another weight, W_R, to set the overall repulsive importance, and by the occupancy probability, E_{oc}. This score is then summed with the scores from the other occupied grid elements, with the final form of this calculation given in Eq. 6. Note that the weights W_{TTC} and W_R are indexed and can be set uniquely on a per-obstacle basis. Additionally, once all of the occupied elements have been checked and their scores summed for the velocity in question, the final score is multiplied by the square of the configuration grid resolution in order to normalize the cost with respect to grid resolution.

$$cost[\vec{v}_r] = res_c^2 \sum_{i=1}^{N} W_{R,i}\left(\frac{W_{TTC,i}}{TTC_{VOS,i}} + \frac{1}{CD_i}\right)E_{oc,i} \tag{6}$$

The shape of this repulsive area is similar to a cone, as shown in Fig. 6. Then, a score is computed that signifies how well that velocity will lead towards the goal– the attractive cost. This involves three terms: one that determines the attractive direction (A_A), one that discourages sudden large direction changes (VD), and one that discourages sudden large accelerations (VC). Within this research, the VD and VC terms were kept as originally stated by Bis et al. [1]. The A_A term, however, was modified in order to improve computational efficiency and programming complexity. This equation was re-written using a dot product, which gives an identical result, as shown in Eq. 7, where $\vec{x}_g$ is the relative location of the goal in velocity space and $\dot{\vec{x}}_g$ is the velocity of the goal.

$$\begin{aligned} \alpha &= \frac{\vec{x}_g + \dot{\vec{x}}_g}{\left\|\vec{x}_g + \dot{\vec{x}}_g\right\|} \cdot \frac{\vec{v}_r}{\|\vec{v}_r\|} \\ A_A &= \begin{cases} -\alpha & \text{if} \quad \alpha > 0 \\ 0 & \text{otherwise} \end{cases} \end{aligned} \tag{7}$$

In addition to the three terms mentioned above, two values are used to set the relative weight between the terms: W_{VD} for VD and W_{AA} for A_A. The attractive cost is designed to be negative for all velocities that would lead towards the goal. A representative example of the final attractive cost is shown in Fig. 7.

$$A_{cost} = VC + W_{VD} \cdot VD + W_{AA} \cdot A_A \tag{8}$$

The process of computing the repulsive cost and the attractive cost is performed over every reachable velocity. These two costs are added to give a map of costs associated with each velocity, as shown in Fig. 8. This map is scanned for the velocity that has the lowest cost and that velocity is selected as the desired robot velocity for the next time step. The minimum cost is shown in Fig. 8 with the bolded outline. Also note how the selected velocity does not lie within the region influenced by the obstacle's repulsive cost.

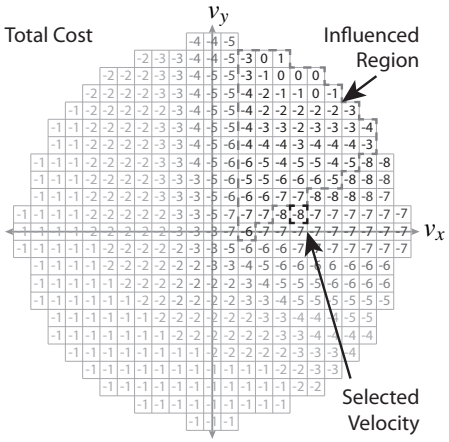

Figure 8: TOTAL COST FOR VELOCITY CHOICE. ONLY PART OF THE TOTAL FIELD IS INFLUENCED BY THE OBSTACLE'S REPULSIVE COST. THE VELOCITY WITH THE LOWEST COST IS SELECTED FOR THE NEXT TIME STEP.

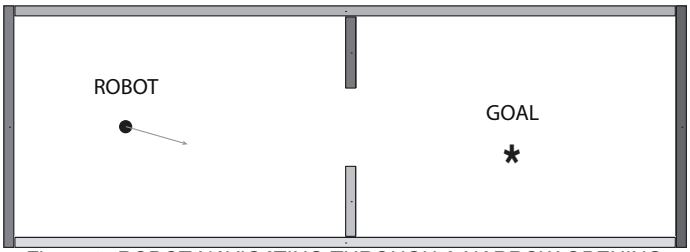

Figure 9: ROBOT NAVIGATING THROUGH A NARROW OPENING.

Therefore, the cost calculation, including the calculation that determines whether or not a velocity will lead to a collision for detected obstacle elements, is crucial to successful obstacle avoidance.

Simulation A suite of scenarios was generated to test the performance of VOS around humans. These scenarios were generated with the intent of mimicking real-life scenarios. Two typical scenarios were selected: traveling parallel to obstacles and pedestrians, like a sidewalk or hall, and perpendicular, like an intersection. In addition, walls surrounding the intended operating area were either included or excluded to impose an additional constraint on the motion and to present large continuously visible obstacles to the robot. Over one thousand scenarios based on combinations of these constraints were generated for testing VOS and pedestrian avoidance.

Additionally, a set of tests was performed with only stationary obstacles set in a doorway configuration, Fig. 9, to determine the minimum door width that VOS could successfully navigate. This was motivated by the need for robots to navigate through buildings. The scenario was also tested treating the boundary of the opening as a human, to simulate the situation in which VOS must pass between two people.

For each scenario, obstacles were placed randomly within a specific region, as shown in Fig. 10. These obstacles were assigned random velocities to yield a trajectory that will interfere

Figure 10: TYPICAL SCENARIO USED FOR EVALUATION.

Table 1: SIMULATION PARAMETERS USED IN ALL SCENARIOS.

Variable	Value
Sensor Range	20 m
Sensor Angular Resolution	0.25°
Sensor Range Resolution	0.2 m
Robot Size	1 m
Maximum Robot Speed	2 m/s
Maximum Robot Acceleration	1 m/s^2
Occupancy Grid Resolution	0.2 m
Velocity Space Resolution	0.05 m/s
Motor Time Step	1 sec
Sensor Time Step	0.1 sec

with the robot. The number of obstacles and their size was also randomized. As many as ten moving obstacles were present in each scenario with the obstacles having x and y dimensions from 1 to 3 m. Obstacles traveling in parallel with the robot were set to have a speed between 0.5 m/s and 2 m/s, with the robot having a maximum speed of 2 m/s. Perpendicular obstacles were set to have a speed between 0.5 m/s and 0.7 m/s so that they would be on an approximate collision course with the robot. The hallway walls were set so the interior was 10 m wide and the total length was set to 110 m. This is a fairly narrow hallway, relative to the robot and obstacle size, so the robot was able to see both sides at all times, restricting its motion. The length was set to allow enough time for the robot to reach maximum velocity before encountering most obstacles. These criteria ensure a complex environment with restricted motion and fast relative velocities (up to 4 m/s). Some of the parameters for the simulation, such as robot size, are fixed over all the simulations and are listed in Table 1. The goal was positioned randomly according to the scenario arrangement and was stationary.

The baseline weights are listed in Table 2. These were derived from the optimal weights as found by Bis et al. [1]. The overall repulsive weight, W_R was increased to compensate for the occupancy space resolution normalization performed in Eq. 6. In addition, the attractive weights were held constant through all of the simulations.

ADJUSTMENT FOR HUMANS

Repulsive Weight

Since VOS selects the velocity with the smallest cost for the next time step, the most intuitive approach is to increase the repulsive weight. That way, VOS would be forced to select a velocity

Table 2: BENCHMARK ATTRACTIVE AND REPULSIVE WEIGHTS. THESE WEIGHTS WERE USED AS A BASELINE FOR PERFORMANCE COMPARISONS.

	Weight	Value
Repulsive Weights	W_{TTC}	3.5
	W_R	30
	W_{AR}	1
	Growth	1
Attractive Weights	W_{VD}	3.5
	W_{AA}	2.2

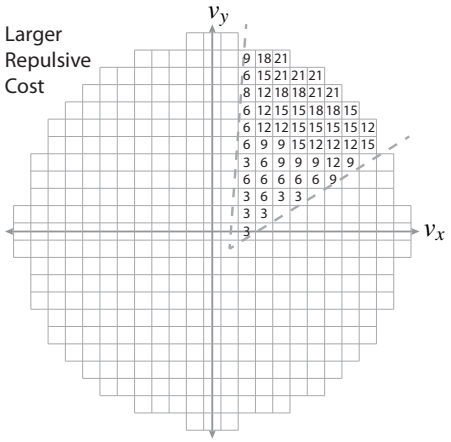

Figure 11: APPLYING A LARGER REPULSIVE COST FOR AN OBSTACLE.

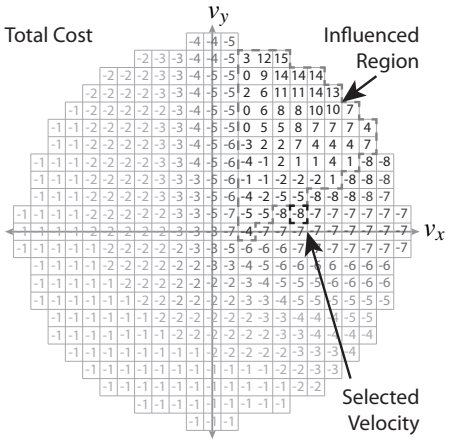

Figure 12: THE TOTAL COST IF A LARGER REPULSIVE WEIGHT IS USED.

that points further away from the obstacle. Knowing this, and looking at Eq. 6, the first reaction would be to increase W_{TTC} so that a larger emphasis is placed on making TTC as large as possible, or to increase W_R so that the overall repulsive cost is increased. An example of this would look like Fig. 11. Unfortunately, this does not have the desired effect. When calculating the repulsive cost, VOS first determines if the velocity in question could lead to a collision, Eq. 2. If it meets the criteria, and only then, the repulsive cost is non-zero. The repulsive cost is added to the attractive cost (which is negative) to produce the total cost shown in Fig. 12. Note that the selected velocity is the same as before. This is because the velocity with the lowest cost was outside of the region influenced by the obstacle. So, despite tripling the repulsive weighting of the obstacle, the velocity chosen is identical. It is possible, though, that the originally selected velocity in Fig. 8 could be within the influenced region if the attractive cost and repulsive cost are carefully balanced. Then, by increasing the repulsive weight of an obstacle, it is possible to push the selected velocity to just outside of the influenced region. Note, however, that it is not possible to alter the velocity choice once it is outside that region.

Increasing Trajectory Criteria Width

Therefore, to choose a significantly different velocity, the region of influence of the obstacle must be enlarged. The first step is to look at the trajectory criteria as described earlier since that determines which velocities will have non-zero repulsive cost. From the relative velocity, an offset, $\vec{p}$, is computed as given in Eq. 1. The offset magnitude, P_A, is composed of the relative position, sensor range, and a weight, W_{AR}, as given in Eq. 3. Increasing the size of P_A, the width of the trajectory criteria, as defined in Eq. 2, will widen the region. By widening the influenced region, the selected velocity can be moved further away from the obstacle. To do this, W_{AR} is increased, which scales P_A. An example of how this widens the trajectory criteria is shown in Fig. 13. As before, this repulsive cost is added to the attractive cost to compute the total cost, as shown in Fig. 14. Note that a different velocity is selected, unlike the case where an increased repulsive weight is used. Therefore, by widening the

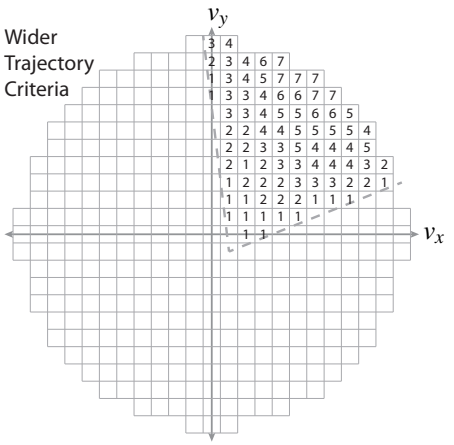

Figure 13: INCREASING THE WIDTH OF THE TRAJECTORY CRITERIA BY INCREASING W_{AR}.

trajectory criteria, it is possible to widen the region of influence and change the velocity choice. This can be a very sensitive change, however. For example, the width in Fig. 13 was made slightly larger, shown in Fig. 15. This only caused two additional velocities to fall within the influenced region and with only a

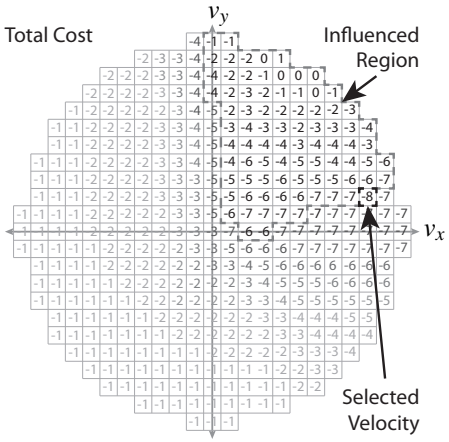

Figure 14: INCREASING THE WIDTH OF THE TRAJECTORY CRITERIA INCREASES THE REGION INFLUENCED BY THE OBSTACLE.

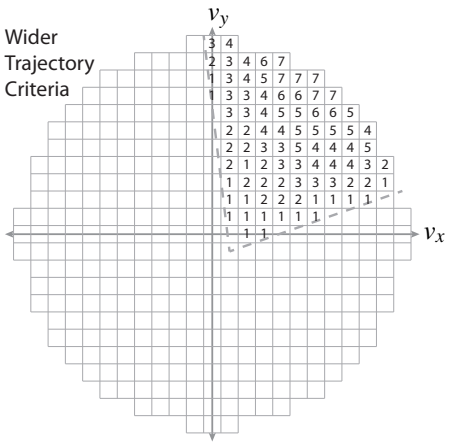

Figure 15: INCREASING THE WIDTH OF THE TRAJECTORY CRITERIA SLIGHTLY MORE.

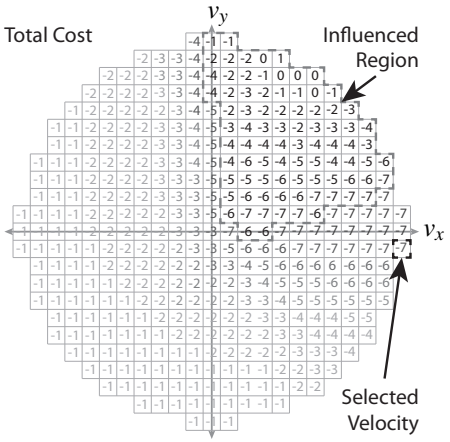

Figure 16: INCREASING THE WIDTH OF THE TRAJECTORY CRITERIA SLIGHTLY MORE INCREASES THE REGION INFLUENCED BY THE OBSTACLE. BUT, THIS RESULTS IN A VERY DIFFERENT VELOCITY CHOICE.

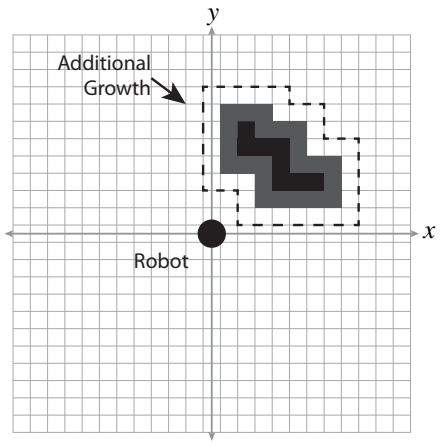

Figure 17: ILLUSTRATION OF ARTIFICIAL GROWTH AROUND PEDESTRIANS.

small repulsive cost. Note, however, that when the total cost is computed, Fig. 16, the selected velocity is very different from before. This is an extreme example, since the costs are integers, however it is possible for such a situation to occur in some cases.

Artificial Growth of Perceived Obstacle

A third method to influence the velocity choice is to increase the perceived size of the obstacle. Instead of only growing the obstacle by the size of the robot, as in Fig. 5, the obstacle is grown by multiples of the robot size. By artificially growing the obstacle, VOS will avoid a larger area. This means that the minimum distance and TTC will increase as VOS will be forced to stay further away and choose velocities that head further from the real obstacle. A visualization of the artificial growth is given in Fig. 17. The resulting repulsive cost is similar to that of the wider trajectory criteria presented in Figs. 13 and 15. This implies that the two techniques have similar effects.

RESULTS

From this analysis of VOS, three potential techniques could be used to change the avoidance behavior around humans: the repulsive cost can be increased, the trajectory criteria can be widened, and the perceived size of the obstacle can be artificially increased. We can see how the performance varies by sweeping the controlling parameter for each of these techniques. A summary of these sweeps looking at their impact on collisions are shown in Figs. 18 and 19. Simulations were run over 1100 random scenarios and basic TTC and CD measurements were made, as summarized in Table 3. The results show that it is possible to improve the avoidance with respect to fewer collisions and increased distance using the techniques described in this paper. The results also show that trying to increase the avoidance around the pedestrian too much can lead to degraded performance with respect to the other obstacles.

Additionally, a narrow opening situation, Fig. 9, was explored. The minimum required opening was found, and the results are shown in Fig. 20. Increasing the trajectory criteria width

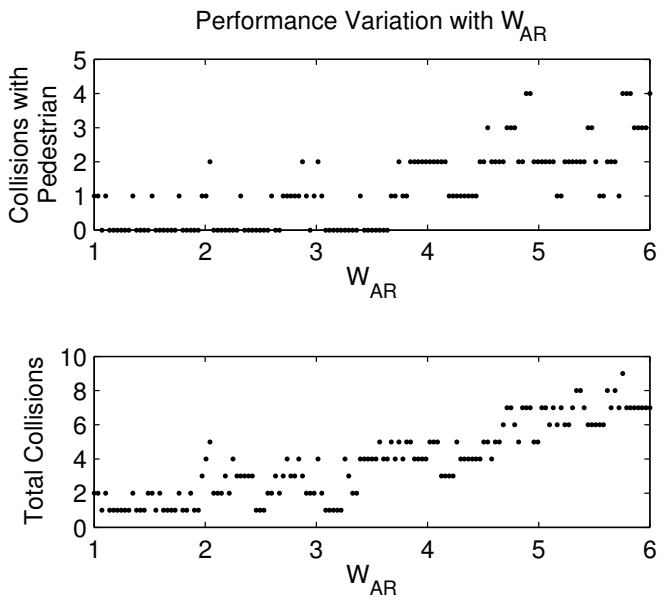

Figure 18: PERFORMANCE VARIATION AS W_{AR} INCREASES. BENCHMARK $W_{AR} = 1$.

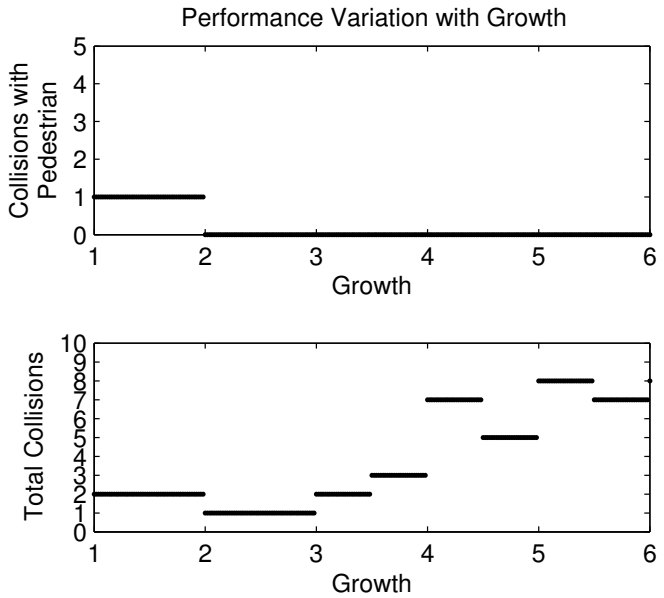

Figure 19: PERFORMANCE VARIATION AS GROWTH INCREASES. BENCHMARK GROWTH = 1. GROWTH IS GIVEN AS MULTIPLES OF THE ROBOT SIZE.

caused the largest increase in necessary opening size, which could easily restrict the movement through confined areas. Artificial growth of obstacles also showed an increase in necessary opening width, however, it did not increase as dramatically.

SUMMARY AND CONCLUSIONS

In this paper, we demonstrated three techniques for adjusting VOS around humans. Two of the techniques, widening the trajectory criteria and artificially growing the obstacle, are capable of adjusting the trajectory significantly. Both can be used to improve the safety and comfort of pedestrians, by nearly doubling the TTC. Additionally, the TTC is closer to human interactions as shown in Fig. 1 However, as the trajectory width and artificial growth increase their influence, performance can suffer as the number of collisions with other obstacles will increase. Widening of the trajectory criteria also shows an increase in number of collisions with the pedestrian as it is made wider, and the performance is very sensitive to small changes in W_{AR}. For the narrow openings, the wider trajectory criteria shows a dramatic increase in the minimum required opening size. The artificial growth also requires a wider opening, however the required width has a stronger dependence on the robot size. Artificial growth shows the most consistent performance across the tested range, and it was able to reduce the collisions with the pedestrian and keep them low.

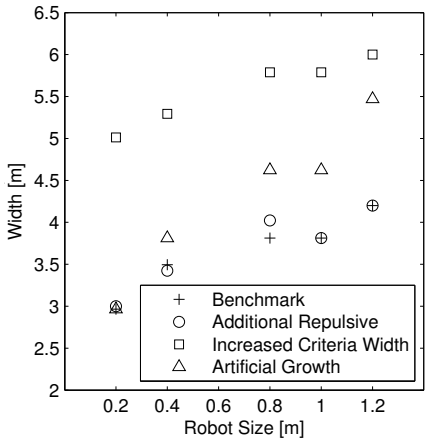

Figure 20: MINIMUM REQUIRED APERTURE WIDTH AS ROBOT SIZE AND AVOIDANCE TECHNIQUE VARY.

Table 3: THE BASE CONFIGURATION AND THREE AVOIDANCE TECHNIQUES (ADDITIONAL REPULSIVE, AR; WIDER TRAJECTORY CRITERIA, W.T.C.; ADDITIONAL GROWTH, A.G.) WERE RUN OVER A SET OF 1100 RANDOM SCENARIOS.

Random Scenarios, N=1100					
		Base	A.R.	W.T.C.	A.G.
Collisions with Pedestrians		1	1	0	0
Total Collisions		3	4	2	2
Minimum TTC with Pedestrian [sec]	Avg	16.1	16.2	16.4	17.1
	Min	0.8	0.8	1.9	2.2
Minimum CD with Pedestrian [m]	Avg	6	6	6.5	6.3
	Min	1.2	1.1	2.2	2.1
Average Computation Time [ms]	Avg	34.6	33.8	34.4	36.7

In conclusion, based on the performance, sensitivity, and required opening size, enhancement using artificial growth is recommended. For future uses of VOS in situations containing pedestrians, the growth method should be used as a starting point to enforce pedestrian safety and comfort. Future work should include experimental testing and integration of a pedestrian detection algorithm to verify that the enhancements demonstrated in simulation perform well in real scenarios. Additionally, VOS could be coupled with a high-level path planning algorithm to demonstrate the full potential of VOS in a practical application.

ACKNOWLEDGMENT

This research was supported in part by the Ground Robotics Reliability Center (GRRC) at the University of Michigan, with funding from government contract DoD-DoA W56H2V-04-2-0001 through the Ground Vehicle Robotics group at TARDEC.

REFERENCES

[1] Bis, R., Peng, H., and Ulsoy, A. G., 2012. "Velocity Occupancy Space: Autonomous Navigation in an Uncertain, Dynamic Environment". *International Journal of Vehicle Autonomous Systems*. In press.

[2] Bis, R., Peng, H., and Ulsoy, A. G., 2009. "Velocity Occupancy Space: Robot Navigation and Moving Obstacle Avoidance with Sensor Uncertainty". In Proceedings of ASME Dynamic Systems and Control Conference.

[3] Hall, E. T., 1966. *The Hidden Dimension*. Doubleday, Garden City, NY.

[4] Hall, E. T., 1968. "Proxemics". *Current Anthropology,* **9**(2-3), pp. 83–108.

[5] Walters, M. L., Dautenhahn, K., te Boekhorst, R., Koay, K. L., Syrdal, D. S., and Nehaniv, C. L., 2009. "An Empirical Framework for Human-Robot Proxemics". In AISB2009: Proceedings of the Symposium on New Frontiers in Human-Robot Interaction, pp. 144–149.

[6] van Oosterhout, T., and Visser, A., 2008. "A Visual Method for Robot Proxemics Measurements". In Proceedings of Metrics for Human-Robot Interaction: A workshop at the Third ACM/IEEE International Conference on Human-Robot Interaction (HRI08), pp. 61–68.

[7] Pacchierotti, E., Christensen, H. I., and Jensfelt, P., 2005. "Human-robot embodied interaction in hallway settings: a pilot user study". In IEEE International Workshop on Robot and Human Interactive Communication, 2005. ROMAN 2005, pp. 164–171.

[8] Koay, K. L., Dautenhahn, K., Woods, S. N., and Walters, M. L., 2006. "Empirical results from using a comfort level device in human-robot interaction studies". In Proceedings of the 1st ACM SIGCHI/SIGART conference on Human-robot interaction, HRI '06, pp. 194–201.

[9] Sisbot, E. A., Marin, L. F., Alami, R., and Siméon, T., 2006. "A mobile robot that performs human acceptable motions". *IEEE/RSJ International Conference on Intelligent Robots an Systems*, pp. 1811–1816.

[10] Shi, D., Jr, E. G. C., Donate, A., Liu, X., Goldiez, B., and Dunlap, D., 2008. "Human-Aware Robot Motion Planning with Velocity Constraints". *International Symposium on Collaborative Technologies and Systems*, May, pp. 490–497.

[11] Gérin-Lajoie, M., Richards, C. L., Fung, J., and McFadyen, B. J., 2008. "Characteristics of personal space during obstacle circumvention in physical and virtual environments". *Gait & Posture,* **27**(2), February, pp. 239–247.

[12] Fink, P. W., Foo, P. S., and Warren, W. H., 2007. "Obstacle avoidance during walking in real and virtual environments". *ACM Transactions on Applied Perception,* **4**, January.

[13] Yoda, M., and Shiota, Y., 1996. "Analysis of human avoidance motion for application to robot". In Robot and Human Communication, 1996., 5th IEEE International Workshop on, pp. 65–70.

[14] Yoda, M., and Shiota, Y., 1997. "The mobile robot which passes a man". In Proceedings of 6th IEEE International Workshop on Robot and Human Communication. RO-MAN'97 SENDAI, pp. 122–117.

[15] Butler, J. T., and Agah, A., 2001. "Psychological Effects of Behavior Patterns of a Mobile Personal Robot". *Autonomous Robots,* **10**, pp. 185–202.

[16] Minh, C. C., Sano, K., and Matsumoto, S., 2005. "Characteristics of passing and paired riding maneuvers of motorcycle". *Journal of the Eastern Asian Society for Transportation Studies,* **6**, pp. 186–197.

[17] Khan, S. I., and Raksuntorn, W., 2001. "Characteristics of Passing and Meeting Maneuvers on Exclusive Bicycle Paths". *Transportation Research Record: Journal of the Transportation Research Board,* **1776**(01-2982), pp. 220–228.

[18] Hoffmann, E. R., and Mortimer, R. G., 1994. "Drivers' Estimates of Time to Collision". *Accident Analysis and Prevention,* **26**(4), August, pp. 511–520.

[19] Bis, R., 2009. Detection and Avoidance of Pedestrians: Review of Existing Literature, April.

[20] Gerónimo, D., López, A. M., Sappa, A. D., and Graf, T., 2010. "Survey of Pedestrian Detection for Advanced Driver Assistance Systems". *IEEE Transactions on Pattern Analysis and Machine Intelligence,* **32**(7), July.

[21] Enzweiler, M., and Gavrila, D. M., 2009. "Monocular Pedestrian Detection: Survey and Experiments". *IEEE Transactions on Pattern Analysis and Machine Intelligence,* **31**(12), December, pp. 2179–2195.

[22] Dalal, N., and Triggs, B., 2005. "Histograms of Oriented Gradients for Human Detection". In Proceedings of IEEE Conference on Computer Vision and Pattern Recognition, Vol. 1, pp. 886–893.